

Identifying pressure dependent elastance in lung mechanics with reduced influence of unmodelled effects

Bernhard Laufer*, Paul D. Docherty**, Yeong Shiong Chiew**,
Knut Möller* and J. Geoffrey Chase**

* *Institute of Technical Medicine (ITeM), HFU Furtwangen University, Villingen-Schwenningen, Germany*
(email: bernhard.laufer@hs-furtwangen.de, moe@hs-furtwangen.de)

** *Department of Mechanical Engineering, University of Canterbury, Christchurch, New Zealand*
(e-mail: paul.docherty@canterbury.ac.nz, yeongshiong.chiew@pg.canterbury.ac.nz,
geoff.chase@canterbury.ac.nz)

The selection of optimal positive end expiratory pressure (PEEP) levels during ventilation therapy of patients with ARDS (acute respiratory distress syndrome) remains a problem for clinicians. One particular mooted strategy states that minimizing the energy transferred to the lung by mechanical ventilation could potentially be used to determine the optimal PEEP level. This minimization could potentially be undertaken by finding the minimum range of dynamic elastance.

In this study, we compare an adapted Gauss-Newton method with the typical gauss newton method in terms of the level of agreement obtained in elastance-pressure curves across different PEEP levels in 10 patients. The Gauss-Newton adaptation effectively ignored characteristics in the data that are un-modelled. The adapted method successfully determined regions of the data that were un-modelled, as expected. In ignoring this un-modelled behavior, the adapted method captured the desired elastance-pressure curves with more consistency than the typical least-squares Gauss Newton method.

Keywords: Gauss-Newton, Physiological Modeling, First order model, Mechanical Ventilation

1. INTRODUCTION

Many studies have been carried out to determine the optimal mechanical ventilation settings (Amato *et al.* 1998). In particular, the selection of the optimal positive end expiratory pressure (PEEP) level remains a challenge in the treatment of patients with acute respiratory distress syndrome (ARDS) (Donahoe 2011; Halter *et al.* 2003; Silversides and Ferguson 2013). Physiological modelling of the lung is one way to determine the best possible settings for mechanical ventilation.

A simple model to describe the respiratory behaviour of the lung is a first order model (FOM) (Cobelli 2008). In this model, the airway passage is symbolized by a single constant resistance term and the tissue resistance to expansion is described by a constant elastance term. The FOM equation is shown in Eq. 1.

$$P = EV + R\dot{V} + P_0 \quad (1)$$

where: P is the airway pressure, P_0 is the offset pressure, V is the volume, \dot{V} is the flow, R is the respiratory system resistance and E is the respiratory system elastance.

The FOM offers modelling simplicity at the cost of descriptive ability and thus cannot capture all pressure flow characteristics of the breathing process. Bates *et al.* (Bates 2009) refers to two different strategies to counter that problem, either the increase in complexity of the model or introduction of nonlinear parameters. A modification of the FOM includes a non-linear time-variant dynamic elastance

$E(t)$ term (Chiew *et al.* 2011; Guttmann *et al.* ; van Drunen *et al.* 2014). $E(t)$ was determined after linear regression identification of the constant R value over a single breath. The time-variant dynamic elastance can also be rewritten as pressure dependent elastance $E(P)$ as shown in Eq. 2.

$$E(P) = \frac{P - P_0 - R\dot{V}}{V} \quad (2)$$

Chiew *et al.* (Chiew *et al.* 2011) utilised a concept of optimal PEEP via the minimization of the respiratory system elastance (Suter *et al.*). Furthermore, Chiew *et al.* showed that this elastance energy is correlated to the work transferred to the lung. Therefore, a well-supported assumption was made that the optimal PEEP level can be set in the region of the tidal pressure where the minimum of the $E(P)$ curve appears. Subsequent studies modelled the $E(P)$ across different PEEP-levels to obtain a continuous prediction curve (Knörzer 2014; Laufer 2015) where their overall goal was to find the minimal $E(P)$ using different extensions to the FOM. This analysis further investigates a volume correction method (V-method) that determines $E(P)$ in concert with R across a number of breaths and PEEP levels and was initially hypothesised by Laufer (2015).

2. METHODS

This study used data from Bersten *et al.* (1998). The data consists of 10 ARDS patients ventilated in square wave flow, volume controlled mode at different PEEP levels. At the end of each PEEP level, patients were ventilated for some time with ZEEP (Zero End Expiratory Pressure) before the next

PEEP level was applied. The last breathing cycles before the PEEP changes were analysed in this study.

It was observed that the elastance-pressure curves were offset from one another across PEEP levels – most likely due to recruitment. Hence, correction terms were applied to the model (Eq. 2). The V-method introduced a variable volume correction term (V_i) for each PEEP level ($P_{0,i}$) and was represented by Eq. 3.

$$E(P) = \frac{P - P_{0,i} - R\dot{V}}{V + V_i} \quad (3)$$

Changes in V_i effectively shifts recruitment and distension characteristics on the $E(P)$ curve. The model shown in Eq. 2 was optimized directly by reducing the disagreement in $E(P)$ across PEEP levels and breaths for each patient. Eq. 4 shows the optimization goal:

$$[V_1, \dots, V_m]_{opt} = \min \left(\sum_{i=1}^{n-m} \sum_{j=i+1}^{n-m} \sum_{P=P_{ij,min}}^{P_{ij,max}} (E(0.1[10P_i]) - E(0.1[10P_j]))^2 \right) \quad (4)$$

Eq. 4 was evaluated on where 2 airway pressure curves of different PEEP overlap ($P \in [P_{ij,min}, P_{ij,max}]$). $P_{ij,min}$ and $P_{ij,max}$ were defined as $P_{ij,min} = \max(\min(P_i), \min(P_j))$ and $P_{ij,max} = \min(\max(P_i), \max(P_j))$. $P_{0,i}$ was the offset pressure (PEEP level) ($i = 1 \dots m$), m was the number of PEEP levels, n was the number of analysed breaths per PEEP level (in this case, $n = 1$ breathing cycle) and the V_i were the volume correction factors. $[x]$ indicates rounding down to the next integer and thus the optimization was conducted in bins with a width of 0.1 cmH₂O.

Two parameter identification strategies were used to identify V_i . The first strategy utilized Levenberg-Marquardt lsqnonlin.m function in MATLAB® 2013a (MathWorks, USA), which matched the $E(P)$ curves only in the end inspiratory pressure range of the $E(P)$ curve of the lower PEEP setting. The parameters of the V-method were identified by minimizing the difference between $E(P)$ levels across PEEP levels of the 20 data points that corresponded to the highest pressure reached at the lower PEEP setting (on the range of $[EIP_i^*, EIP_i]$). This method will be referred to as ‘trend fitting’ and is represented in Eq. 5.

$$[V_1, \dots, V_m]_{opt} = \min \left(\sum_{i=0}^{m-1} \sum_{P=EIP_i^*}^{EIP_i} (E(0.1[10P_i]) - E(0.1[10P_{i+1}]))^2 \right) \quad (5)$$

The second strategy was to optimize Eq. 5 using an adapted Gauss-Newton (GN) algorithm, introduced by Gray *et al.* (Docherty *et al.*; Gray *et al.*). This approach was designed to reduce the influence of outlier data or un-modelled characteristics on the outcomes of model-based analysis. The GN method iterates the parameter vector according to Eq. 6.

$$\mathbf{x}_{i+1} = \mathbf{x}_i - (\mathbf{J}^T \mathbf{J})^{-1} \mathbf{J}^T \boldsymbol{\psi} \quad (6)$$

where \mathbf{x} is the vector of parameters to be identified, $\boldsymbol{\psi}$ is the residual vector and \mathbf{J} is the Jacobian:

$$\mathbf{x} = \begin{pmatrix} V_1 \\ \vdots \\ V_m \end{pmatrix}; \boldsymbol{\psi} := \begin{pmatrix} \sum_{i=1}^{n-m} \sum_{j=i+1}^{n-m} |E_i(P_1) - E_j(P_1)| \\ \vdots \\ \sum_{i=1}^{n-m} \sum_{j=i+1}^{n-m} |E_i(P_{max}) - E_j(P_{max})| \end{pmatrix};$$

$$\mathbf{J} := \begin{pmatrix} \frac{\partial \psi_1}{\partial V_1} & \dots & \frac{\partial \psi_1}{\partial V_m} \\ \vdots & \ddots & \vdots \\ \frac{\partial \psi_k}{\partial V_1} & \dots & \frac{\partial \psi_k}{\partial V_m} \end{pmatrix} \quad (6^*)$$

Gray *et al.* (2015) modified Eq. 6 by modulating the magnitude of the residual vector and thus changing the weighting given to each data point in the iterations.

$$\mathbf{x}_{i+1} = \mathbf{x}_i - (\mathbf{J}^T \mathbf{J})^{-1} \mathbf{J}^T \hat{\boldsymbol{\psi}} \quad (7)$$

where the modification $\hat{\boldsymbol{\psi}}$ is defined as follows:

$$\hat{\boldsymbol{\psi}} = [\hat{\psi}_j] = \left[\psi_j e^{\left(\frac{-|\psi_j|}{\beta |\hat{\psi}|} \right)} \right] \quad (7^*)$$

where $|\hat{\psi}|$ is the median absolute residual and β is a scaling factor.

After the identification of the correction factors V_i via optimizing the equivalence in the characteristics of the $E(P)$ curves, the $E(P)$ curve indicated an exponential decrease at the beginning followed by a linear increase. This $E(P)$ profile can be captured by a function given by:

$$E_{fit}(P) = a_1 e^{a_2 P} + a_3 P + a_4 \quad (8)$$

This function $E_{fit}(P)$ was fitted to the curve after the optimization using the same adapted Gauss-Newton algorithm and the residual vector was given by

$$\boldsymbol{\psi}(P) = \begin{pmatrix} |E_{fit}(P_1) - E(P_1)| \\ \vdots \\ |E_{fit}(P_{max}) - E(P_{max})| \end{pmatrix} \quad (9)$$

The three methods were compared in their ability to capture consistent patient $E(P)$ curves across different PEEP levels. The three methods were:

- trend fitting (Eq. 5, $[EIP_i^*, EIP_i]$)
- original GN (Eq. 6 - least squares)
- adapted GN (using Eq. 5, full data, least squares and reducing un-modelled effects) applied with different scaling factors ($\beta = 10, 2$ and 1)

Evaluation of the methods is conducted by the level of agreement observed in the $E(P)$ curves, and the repeatability of the optimal PEEP as defined by Eq. 8 in a bootstrapping exercise (repetition of the analysis with random breath omission).

3. RESULTS

Figs. 2 and 3 show the $E(P)$ curves after optimization and the impact of each data point on the optimization results. Fig. 2A shows the original $E(P)$ curves obtained by Eq. 2. The V-method (Eq. 3) was designed to counteract the offset that implies different elastance at different PEEP levels. Fig. 2B shows the results of the trend fitting approach. The trend fitting used only the higher pressure ranges of the data (Eq.

6). This use of high pressure data only can be seen as well in Fig. 2C. $E(P)$ curves optimized according to typical least-squares criteria and the corresponding influences of the data points is shown in Fig. 2D-F. The typical least-squares GN algorithms treat all data points as representative of the modelled behaviour, and thus, all points have an unmodified contribution to the objective function (Fig. 2E-F). A

continuous prediction curve for $E(P)$ could not be obtained.

Fig. 3 shows changes achieved by the application of the adapted GN algorithm using different scaling factors. Figs. 3A-C show the results for $\beta=10$. $\beta=10$ yields no significant changes compared to the original GN algorithm (Fig. 2E compared to Fig. 3B).

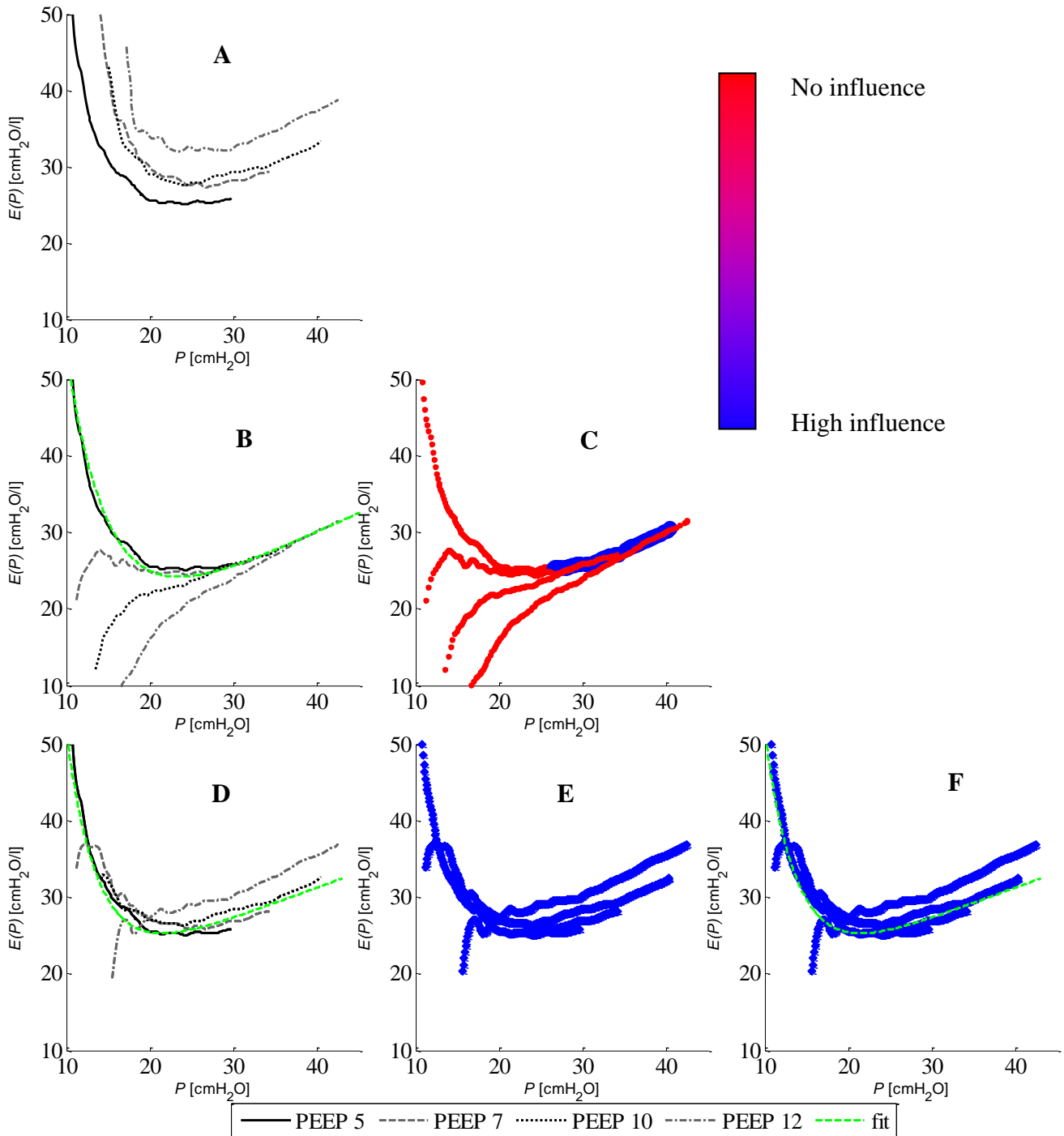


Fig. 2. $E(P)$ curves for Patient 10 using: direct evaluation of Eq. 4 (A); data contribution during trend optimization (B-C); and the weighting of points in the GN method (C); the $E(P)$ curves and their fits using equal weighting of all data (D-F); the contribution of the datapoints towards fitting Eq. 5 (E); and the contribution of the datapoints on fitting to $E_{fit}(P)$ (F)

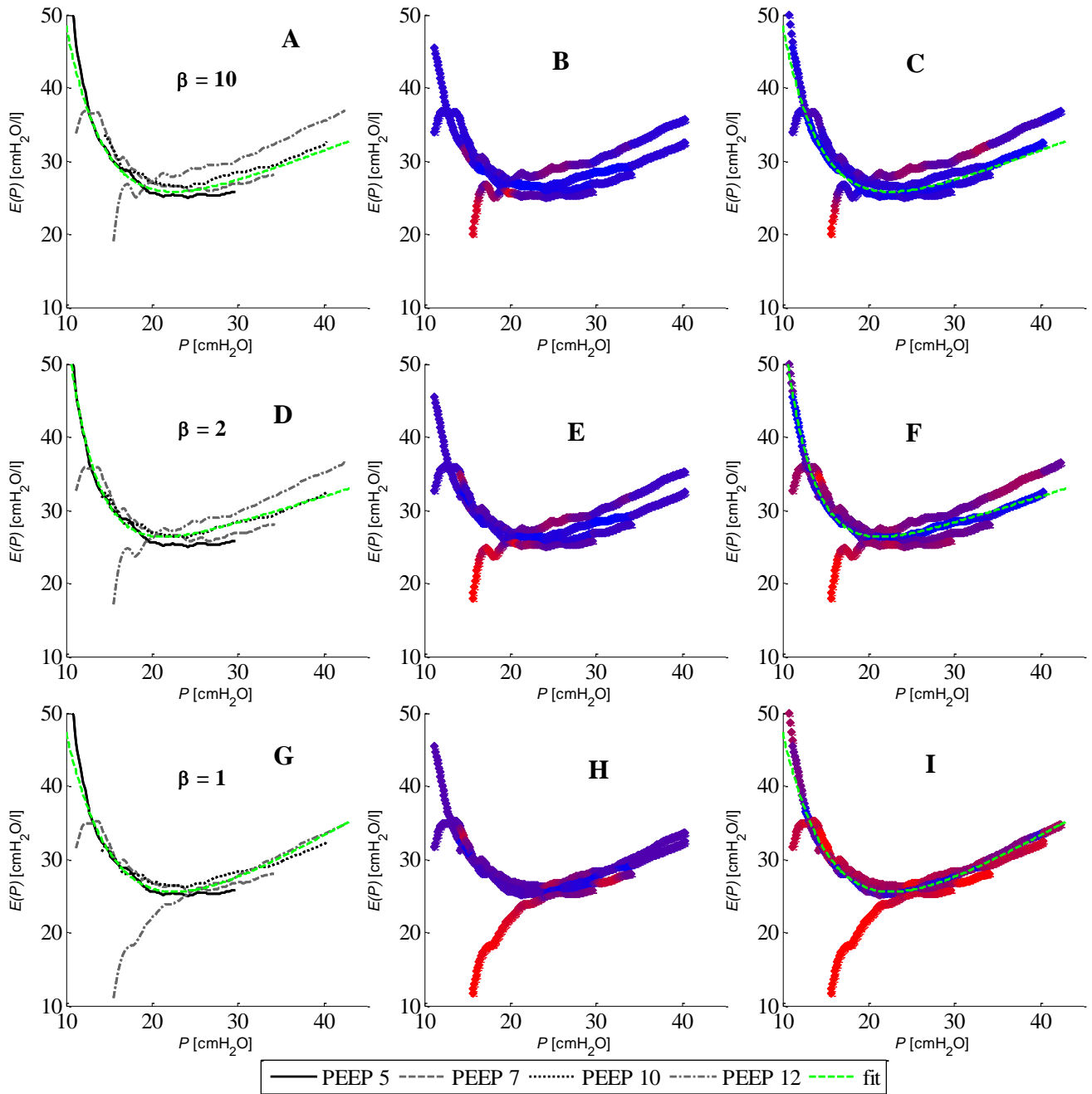


Fig. 3. $E(P)$ curves fits for Patient 10 using the adapted GN method with: $\beta = 10$ (A-C), $\beta = 2$ (D-F) and $\beta = 1$ (G-I). The left figures (A, D, G) show the $E(P)$ simulations for each breath. The central column (B, E, H) shows the contribution of each point towards the minimisation of Eq. 5. The right column of figures (C, F, I) shows the contribution of each data point to the fitting of $E_{fit}(P)$

The changes due to the adaptation of the GN method can be seen for smaller values of β . In particular, in Figs. 3B, 3E and 3H show that the contribution from some poorly captured data points is significantly reduced. Hence, the adapted GN was able to ensure much greater consistency in outcomes for the remainder of the $E(P)$ curves. The advantage of this method can be seen obviously when $\beta=1$. Fig 3I shows that the $E(P)$ curves are very close together for significant periods of the breath cycles when $\beta=1$. However, the corresponding weighting plots demonstrated that this is achieved by a significant reduction in the weighting of the data, that is

distant from the given $E(P)$ curve. Thus the impact of the unmodelled effects is suppressed significantly, and the results are close to the result of the trend fitting method (Fig. 2C). The adherence to the $E_{fit}(P)$ line is much better for the majority of the curve when the β value is at a minimum (Fig. 3H).

Table 1 shows the formulations of $E_{fit}(P)$ (Eq. 8) used to fit the $E(P)$ curves. Fig. 4 shows the distribution of optimal PEEP settings as found via Eq. 8 and the corresponding elastance levels obtained in a bootstrapping analysis of randomly selected breaths.

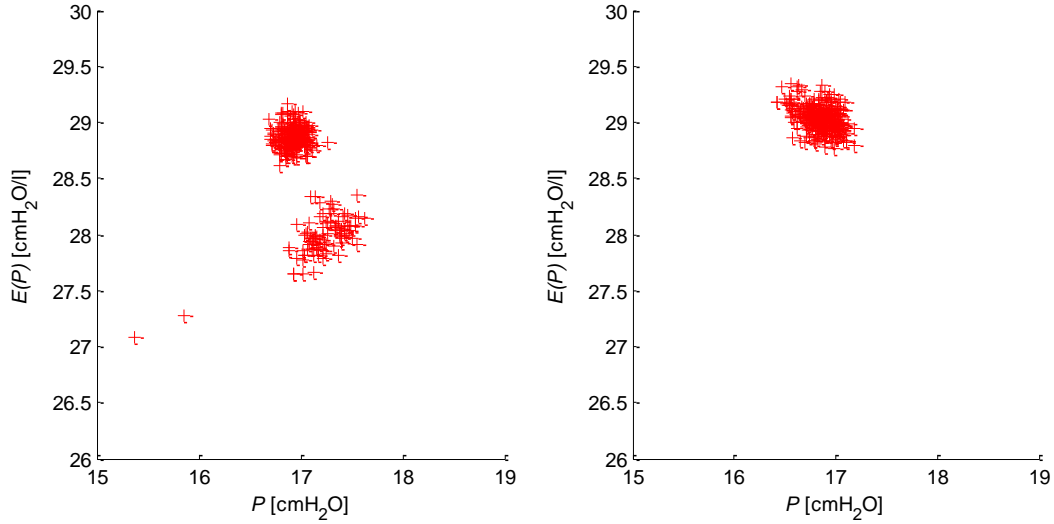


Fig. 4. Optimal PEEP determined by Eq. 8 and the corresponding elastance as determined in a bootstrapping analysis of the standard GN (left) and the adapted GN (right).

Table 1. Eq. 8 fits for Patient 10 using the various curve fitting algorithms

Method	Equation 8
Trend optimization	$E_{fit}(P) = 300e^{-0.21P} - 0.5P + 10$
Gauss Newton ($\beta = \infty$)	$E_{fit}(P) = 470e^{-0.27P} - 0.43P + 15$
Adapted GN ($\beta = 10$)	$E_{fit}(P) = 540e^{-0.27P} - 0.41P + 17$
Adapted GN ($\beta = 2$)	$E_{fit}(P) = 640e^{-0.29P} - 0.36P + 17$
Adapted GN ($\beta = 1$)	$E_{fit}(P) = 190e^{-0.17P} - 0.66P + 7$

4. DISCUSSION

In this analysis, we have presented two methods for determination of a pressure dependent elastance term, $E(P)$. This non-linear curve captures the pressure-volume relationship across PEEP levels. Hence, the $E(P)$ curves fulfil one of the criteria of Bates (Bates 2009) that calls for non-linear parameters to improve the fitting capability of the FOM.

In order for the $E(P)$ curves to describe the same lung physiology across PEEP levels, a volume correction term (V_i) is added. This correction term captures the recruited lung volume that occurs at PEEP steps (Hickling). It is necessary to eliminate volume creep in the numerical integration of flow data. Thus, precise determination of the recruited volume due to PEEP increments is not possible. Hence, the V_i terms are necessary to ensure that the elastance derived is representative of equivalent pressure levels.

The first method presented in this study was the trend fitting algorithm. This method matched the high pressure segments of each breath, and thus was relatively easily implemented. Fig. 2C shows that the unmodelled effects that are present at low pressure intervals of the breath cycle are effectively ignored. However, this means that agreement between the $E(P)$ curves across breaths is only maximised in the high pressure regions of the breath. This does not preclude agreement at low pressures. However, Fig. 2C shows that the level of agreement for Patient 10 reduced significantly

outside of the region that was used in the optimisation set optimisation data (Eq. 5, $[EIP_i^*, EIP_i]$).

In contrast, the adapted GN method had the opportunity to use the entirety of the data set and autonomously determine which data was not modelled by the model (Docherty *et al.*; Gray *et al.*). This method works by first determining a residual profile at the current iteration. Data points that yield residuals considerably further away than the median absolute residual are considered by the algorithm as representative of un-modelled behaviour. The weighting of such data-points is then reduced in the algorithm according the value of β . As iterations progress and the model converges, the magnitude of the residuals reduces and the adapted method effectively tightens the objective surface around the solutions which agrees with the majority of the data points. Figs. 3B, 3E and 3H show what data the method has considered unmodelled.

The value of β is an important setting in the adapted method. In particular, the value of β determines how aggressive the method is in the reduction of the influence of unmodelled effects. Fig. 3B shows that the influence of the low elastance – low pressure segment of one of the breaths is having a significant effect on the outcomes when $\beta=10$. This effect causes a lower level of agreement through the majority of the data in comparison to when $\beta=1$ (Fig. 3H).

Of note, the trend fitting algorithm ignores a similar section of the data as the adapted method when $\beta=1$. However, the key difference is that the adapted method autonomously determines which data could potentially be true to the model. In particular, there is more data contributing to the analysis in Fig. 3H than in Fig. 2C. This means that the $E(P)$ curves determined using the autonomous method are more robust and representative across the breaths and PEEP levels.

Fig. 4 shows that there is greater consistency in the optimal PEEP levels determined via Eq. 8 when using the adapted method compared to the trend fitting method. However, the variance is predominantly in elastance, and not in the key clinical metric of optimal PEEP. This is not entirely

unexpected since Figs. 2C and 3H are optimised on much the same data. Hence, in terms of clinical implementation, the added complexity of the adapted method may not be warranted due to the equivalent outcome produced by the less complex trend fitting method.

This paper presents an analysis of data from a single ARDS patient from the study conducted by Bersten *et al.* (Bersten 1998). However, in data not shown, it was confirmed the outcomes were indicative of the outcomes of the wider dataset of 25 ARDS patients.

Developing a method that effectively ignores unmodelled effects is a contentious concept. Some researchers consider every data point to be valuable and consider methods that reduce the contribution of any points in the objective function to be akin to data manipulation. This paradigm ultimately leads to larger more complex model formulations. The increased complexity of such models is necessary to capture the behaviour that was not modelled by the simple model. However, when such models are applied in the absence of the unmodelled effects, parameter non-identifiability occurs (Docherty *et al.* ; Docherty *et al.* 2014). Hence, by using the adapted method, a determination of precisely which data points can be representative of the modelled behaviour is treated autonomously. This further ensures the operator independence of the method while concurrently limiting the effect of unmodelled effects on the outcomes.

5. CONCLUSIONS

Applying volume correction terms to the simple FOM model yielded improvements to the agreement of the $E(P)$ curves at different PEEP levels. The adapted Gauss-Newton method was introduced for curve fitting processes to while reducing unmodelled effects. This study showed that the adapted method offered increased robustness in $E(P)$ curves. However, the added robustness did not have any particular clinical utility over the simpler trend-fitting algorithm that was also tested. Overall, this approach has the potential to yield information regarding the elastance curves of critically ill patients and to determine optimal PEEP setting that reduce the potential for ventilator induced lung injury.

6. ACKNOWLEDGEMENT

We want to thank for the support through the EU-Sponsorship – “eTime” – ID : “FP7-PEOPLE-2012-IRSES”.

REFERENCES

- Amato M.B.P., Barbas C.S.V., Medeiros D.M., Magaldi R.B., Schettino G.P., Lorenzi-Filho G., Kairalla R.A., Deheinzelin D., Munoz C., Oliveira R., Takagaki T.Y., Carvalho C.R.R. (1998) Effect of a Protective-Ventilation Strategy on Mortality in the Acute Respiratory Distress Syndrome, *N Engl J Med*, 338(6), 347-354
- Bates J.H.T.: *Lung Mechanics: An Inverse Modeling Approach*. United States of America, New York, Cambridge University Press, 2009
- Bersten A.D. (1998) Measurement of overinflation by multiple linear regression analysis in patients with acute lung injury, *Eur Respir J*, 12(3), 526-532
- Chiew Y.S., Chase J.G., Shaw G., Sundaresan A., Desai T. (2011) Model-based PEEP Optimisation in Mechanical Ventilation, *BioMedical Engineering OnLine*, 10(1), 111
- Cobelli C.: *Introduction to modeling in physiology and medicine*. Amsterdam; Boston, Academic Press, 2008
- Docherty P., Chase J.G., Lotz T., Desai T. (2011) A graphical method for practical and informative identifiability analyses of physiological models: A case study of insulin kinetics and sensitivity, *Biomedical Engineering Online*, 10(39),
- Docherty P.D., Gray R.A.L., Mansell E.: Reducing the Effect of Outlying Data on the Identification of Insulinaemic Pharmacokinetic Parameters with an Adapted Gauss-Newton Approach. In *IFAC 19th World Congress* Boje E, Ed. Cape Town, South Africa, 2014
- Docherty P.D., Schranz C., Chiew Y.-S., Möller K., Chase J.G. (2014) Reformulation of the pressure-dependent recruitment model (PRM) of respiratory mechanics, *Biomedical Signal Processing and Control*, 0),
- Donahoe M. (2011) Acute respiratory distress syndrome: A clinical review, *Pulmonary Circulation*, 1(2), 192-211
- Gray R.A.L., Docherty P.D., Fisk L.M. (2015) A modified approach to objective surface generation within the Gauss-Newton parameter identification to ignore outlier data points., *Med. Biol. Eng. Comput.*, In review(
- Guttmann J., Eberhard L., Fabry B., Zappe D., Bernhard H., Lichtwarck-Aschoff M., Adolph M., Wolff G. (1994) Determination of volume-dependent respiratory system mechanics using the new SLICE method, *Technology and Health Care*, 2(3), 175-191
- Halter J.M., Steinberg J.M., Schiller H.J., DaSilva M., Gatto L.A., Landas S., Nieman G.F. (2003) Positive End-Expiratory Pressure after a Recruitment Maneuver Prevents Both Alveolar Collapse and Recruitment/Derecruitment, *Am J Respir Crit Care Med*, 167(12), 1620-1626
- Hickling K.G. (1998) The Pressure-Volume Curve Is Greatly Modified by Recruitment: A Mathematical Model of ARDS Lungs, *American Journal of Respiratory and Critical Care Medicine*, 158(1), 194-202
- Knörzer A.D., P.D.; Chiew, Y.S.; Chase, J.G.; Möller, K. (2014) An Extension to the First Order Model of Pulmonary Mechanics to Capture a Pressure dependent Elastance in the Human Lung, *Conference paper to 19th IFAC World Congress*,
- Laufer B.K., A.; Docherty, P.D.; Chiew, Y.S.; Chase, J.G.; Möller, K. (2015) Performance of variations of the dynamic elastance model in lung mechanics, *unpublished*,
- Silversides J., Ferguson N. (2013) Clinical review: Acute respiratory distress syndrome clinical ventilator management and adjunct therapy, *Crit Care*, 17(2), 225
- Suter P.M., Fairley H.B., Isenberg M.D. (1975) Optimum End-Expiratory Airway Pressure in Patients with Acute Pulmonary Failure, *New England Journal of Medicine*, 292(6), 284-289
- van Drunen E., Chiew Y.S., Pretty C., Shaw G., Lambermont B., Janssen N., Chase J., Desai T. (2014) Visualisation of time-varying respiratory system elastance in experimental ARDS animal models, *BMC Pulmonary Medicine*, 14(1), 33